International Journal of Heat and Mass Transfer 96 (2016) 29–41

Contents lists available at ScienceDirect

International Journal of Heat and Mass Transfer

journal homepage: www.elsevier.com/locate/ijhmt

Comparative study of the Boltzmann and McCormack equations for Couette and Fourier flows of binary gaseous mixtures

Minh Tuan Ho [a,1], Lei Wu [b], Irina Graur [a,*], Yonghao Zhang [b], Jason M. Reese [c]

[a] Aix-Marseille Université, CNRS, IUSTI UMR 7343, 13453 Marseille, France
[b] James Weir Fluids Laboratory, Department of Mechanical and Aerospace Engineering, University of Strathclyde, Glasgow G1 1XJ, UK
[c] School of Engineering, University of Edinburgh, Edinburgh EH9 3JL, UK

ARTICLE INFO

Article history:
Received 8 September 2015
Received in revised form 23 December 2015
Accepted 30 December 2015
Available online 21 January 2016

ABSTRACT

We evaluate the accuracy of the McCormack model by comparing its solutions for Couette and Fourier flows of binary gaseous mixtures with results from the linearized Boltzmann equation. Numerical simulations of Ne–Ar and He–Xe gas mixtures are carried out from slip to near free-molecular flow regimes for different values of the molar concentration. Our numerical results show that while there are only small differences in the shear stress in Couette flow and the heat flux in Fourier flow, calculated from the two kinetic equations, differences in other macroscopic quantities can be very large, especially in free-molecular flow regime. Moreover, the difference between results from the two models increases with the molecular mass ratio and the molar concentration of the heavier species. Finally, the applicability of the McCormack model, which was derived for linearized flows only, is investigated by comparing its solutions with those from the Boltzmann equation for Fourier flow with large wall-temperature ratios.

1. Introduction

In practical applications like vacuum technology, porous media, and the chemical industry, information about the heat/mass transfer in rarefied gaseous mixtures is indispensable. Benchmark test cases are of great importance as they can validate new numerical models developed to describe gas flows or test the validity of existing approaches under various physical conditions. In this paper, Couette and Fourier flows between two parallel plates are chosen as benchmark test cases as they are classical problems in fluid mechanics. Although solutions for single-species gases have been well studied, few papers have investigated gaseous mixtures.

The plane Couette flow of a binary gaseous mixture was first studied [1–5] using kinetic models for the Boltzmann equation (BE), such as the Hamel model [6] for Maxwellian molecules and the McCormack model for general intermolecular potentials [7]. Notably, following the McCormack model, the influence of intermolecular interactions on the velocity and shear stress in three mixtures (Ne–Ar, He–Ar, and He–Xe) [4] and the influence of the gas-surface interaction on the flow properties were investigated [5]. The linearized Boltzmann equation (LBE) for hard-sphere (HS) molecules has been solved by an analytical version of the discrete-ordinates (ADO) method [8], and the accuracy of the McCormack model has been assessed for a He–Ar mixture: the McCormack model produces accurate shear stress for each species, and the velocity of the heavier species [5,8]; however, the velocity of the lighter species and especially the heat flux significantly deviate from the LBE results (by over 100% for some case).

Very few papers have tackled the heat transfer through a binary gaseous mixture. Plane Fourier flow was first simulated by solving the BE using the numerical kernel method [9]. Later, the heat transfer between two plates with a small temperature difference was studied using the McCormack model [10] and the LBE [11]. Surprisingly, the normalized heat flux for Ne–Ar and He–Xe mixtures obtained from the linearized equations were found to agree with results from the BE, with the maximum relative deviation being about 4%. However, there were large differences in the density and temperature between the McCormack model and the LBE: for density, up to 15% difference in Ne–Ar mixture and 51% in He–Xe mixture were observed, while for temperature the maximum differences were 12% and 20% for Ne–Ar and He–Xe mixtures, respectively. The influence of intermolecular potentials on the heat flux between two parallel plates, for three binary mixtures of noble gases (Ne–Ar, He–Ar, He–Xe), has been studied using the McCormack model [12]: the heat flux is sensitive to the intermolecular potential, and the difference between the HS and realistic potential [13] reached 15% near the hydrodynamic regime.

To summarize, only two papers have compared the McCormack model and the LBE for mixtures of Ne–Ar, He–Xe [11], and He–Ar

* Corresponding author.
E-mail addresses: minhtuan.ho@etu.univ-amu.fr (M.T. Ho), irina.martin@univ-amu.fr (I. Graur).
[1] Current address: James Weir Fluids Laboratory, Department of Mechanical and Aerospace Engineering, University of Strathclyde, Glasgow G1 1XJ, UK.

http://dx.doi.org/10.1016/j.ijheatmasstransfer.2015.12.068
0017-9310/

[8]. Therefore, systematic new comparisons between the McCormack model and the LBE will be useful for further development of numerical tools for the simulation of gaseous mixture flows. In this paper, Couette and Fourier flows are considered with two types of binary gaseous mixture composition. Different species accommodation coefficients are considered, and their influence on the flow parameters is analyzed. A large temperature difference between the two plates in Fourier flow is also investigated, where the results from the McCormack model are compared with those from the BE in order to establish the limits of the linearized approach.

2. Problem statement

Consider a binary mixture of monatomic gases, where the mass of a molecule of the first (second) species is m_1 (m_2), and the corresponding number density is n_1 (n_2). Without loss of generality, we assume $m_1 < m_2$. The gaseous mixture is confined between two parallel plates situated at $y' = \pm H/2$, see Fig. 1. In Couette flow, the two plates with temperature T_0 move in opposite directions with a speed $U/2$. In Fourier flow, both plates are stationary, but the plate at $y' = -H/2$ has a temperature of $T_C = T_0 - \Delta T/2$, while the other one has $T_H = T_0 + \Delta T/2$. We assume that, in the case of Couette flow, the relative speed of the two plates U is much smaller than the most probable molecular velocity v_0 of the mixture. We also assume that the temperature difference ΔT, in the case of Fourier flow, is much smaller than the equilibrium gas temperature T_0, so the gaseous mixture deviates only slightly from thermodynamic equilibrium and the McCormack model can be applied.

The most probable molecular velocity of the mixture is:

$$v_0 = \sqrt{\frac{2kT_0}{m}}, \tag{1}$$

where k is the Boltzmann constant and $m = C_0 m_1 + (1 - C_0)m_2$ is the mean molecular mass of the mixture. Here, C_0 is the equilibrium molar concentration of the lighter species,

$$C_0 = \frac{n_{01}}{n_{01} + n_{02}}, \tag{2}$$

and $n_{0\alpha}$ is the equilibrium number density of species α ($\alpha = 1, 2$). The equilibrium number density of the mixture is $n_0 = n_{01} + n_{02}$.

In Couette flow, we are interested in the profiles of the species velocity $u'_{\alpha x}$ and shear stress $P'_{\alpha xy}$, while in Fourier flow, we are interested in the deviated density n'_α, concentration $C' = (n_{01} + n'_1)/(n_{01} + n_{02} + n'_1 + n'_2)$, deviated temperature T'_α, and heat flux $q'_{\alpha y}$.

3. Kinetic equations

To describe the gas dynamics at various conditions, the gas kinetic theory is necessary. In this section, the BE for the binary gaseous mixture is first introduced. Then, the McCormack model is used to simplify the Boltzmann collision operator for linearized Couette and Fourier flows. Finally, the gas-wall boundary condition is specified and numerical techniques to solve the kinetic equations are briefly described.

3.1. The Boltzmann equation

Let $f_\alpha(t, x, v)$ be the distribution function of specie α with molecular velocity v at spatial location x and time t. In the absence of external forces, the following BE describes the evolution of f_1 and f_2:

$$\frac{\partial f_\alpha}{\partial t} + v \cdot \frac{\partial f_\alpha}{\partial x} = \sum_{\beta=1,2} Q_{\alpha\beta}(f_\alpha, f_\beta), \tag{3}$$

where the Boltzmann collision operator $Q_{\alpha\beta}(f_\alpha, f_\beta)$ is

$$Q_{\alpha\beta}(f_\alpha, f_\beta) = \int_{\mathbb{R}^3}\int_{\mathbb{S}^2} C_{\alpha\beta}(\theta, |v_r|)\left[f_\beta({}'v_*^{\alpha\beta}) f_\alpha({}'v^{\alpha\beta}) - f_\beta(v_*) f_\alpha(v)\right] d\Omega dv_*. \tag{4}$$

In the above equations, v and v_* are the pre-collision velocities of molecules of species α and β, respectively, while ${}'v^{\alpha\beta}, {}'v_*^{\alpha\beta}$ are the corresponding post-collision velocities. Conservation of momentum and energy yield the following relations: ${}'v^{\alpha\beta} = v + m_\beta(|v_r|\Omega - v_r)/(m_\alpha + m_\beta)$ and ${}'v_*^{\alpha\beta} = v_* - m_\alpha(|v_r|\Omega - v_r)/(m_\alpha + m_\beta)$, where $v_r = v - v_*$ is the relative pre-collision velocity, Ω is the unit vector in the sphere $\mathbb{S}^2$ with the same direction as the relative post-collision velocity, and θ is the deflection angle between the two relative velocities, i.e. $\cos\theta = \Omega \cdot v_r/|v_r|$. Finally, for hard-sphere molecules, the collision kernels $C_{\alpha\beta}$ are given by

$$C_{11} = \frac{d_1^2}{4}|v_r|, \quad C_{22} = \frac{d_2^2}{4}|v_r|, \quad C_{12} = C_{21} = \frac{(d_1 + d_2)^2}{16}|v_r|, \tag{5}$$

where d_α is the molecular diameter of species α.

For systems that only slightly deviate from equilibrium, the BE can be linearized. Introducing the equilibrium Maxwellian distribution function:

$$f_\alpha^M(v) = n_{0_\alpha}\left(\frac{m_\alpha}{2\pi kT_0}\right)^{3/2} \exp\left(-\frac{m_\alpha v^2}{2kT_0}\right), \tag{6}$$

and expressing the (steady-state) distribution function in the form of $f_\alpha(x, v) = f_\alpha^M(v) + f_\alpha^d(x, v)\xi$, where $f_\alpha^d(x, v)$ is the perturbed distribution function, $\xi = U/v_0 \ll 1$ for Couette flow and $\xi = \Delta T/T_0 \ll 1$ for Fourier flow, the LBE becomes

$$v_y \frac{\partial f_\alpha^d}{\partial y} = \sum_{\beta=1,2} L_{\alpha\beta}(f_\alpha^d, f_\beta^d), \tag{7}$$

with the linearized Boltzmann collision operator $L_{\alpha\beta}(f_\alpha^d, f_\beta^d) = Q_{\alpha\beta}(f_\alpha^M, f_\beta^d) + Q_{\alpha\beta}(f_\alpha^d, f_\beta^M)$.

When the perturbation function f_α^d is known, the deviated (from equilibrium values) macroscopic flow quantities of species α, such as the density, velocity, shear stress, temperature, and heat flux, are calculated as follows: $n'_\alpha = \xi\int f_\alpha^d dv, u'_{\alpha i} = \xi\int f_\alpha^d v_i dv/n_{0_\alpha}, P'_{\alpha xy} = m_\alpha\xi\int f_\alpha^d v_x v_y dv$, $T'_\alpha = \xi\int f_\alpha^d(2m_\alpha v^2/3 - 1)dv$, and $q'_{\alpha i} = m_\alpha\xi\int f_\alpha^d v_i (v^2 - 5/2)dv$.

3.2. The McCormack model

The McCormack model was proposed for linearized flows of multicomponent monatomic mixture [7], where the linearized collision operator is obtained by requiring that its first three velocity moments be the same as the corresponding moments of the linearized Boltzmann collision operator. Expressing the distribution function in the form $f_\alpha = f_\alpha^M(v)(1 + h_\alpha\xi)$, the McCormack model for the steady-state solution reads

$$c_{\alpha y}\frac{\partial h_\alpha}{\partial y} = H\sqrt{\frac{m_\alpha}{2kT_0}}\sum_{\beta=1}^{2} L_{\alpha\beta}h, \tag{8}$$

where the linearized collision operator $L_{\alpha\beta}h$ is given in A. Note that in writing Eq. (8), we have used the following dimensionless quantities:

$$y = \frac{y'}{H}, \; c_\alpha = \sqrt{\frac{m_\alpha}{2kT_0}}v, \; n_\alpha = \frac{n'_\alpha}{n_{0\alpha}\xi}, \; u_{\alpha x} = \frac{u'_{\alpha x}}{U}, \; P_{\alpha xy} = -\frac{P'_{\alpha xy}}{2p_{0\alpha}\xi},$$
$$T_\alpha = \frac{T'_\alpha}{T_0\xi}, \; q_{\alpha y} = \frac{q'_{\alpha y}}{p_{0\alpha}v_0\xi},$$

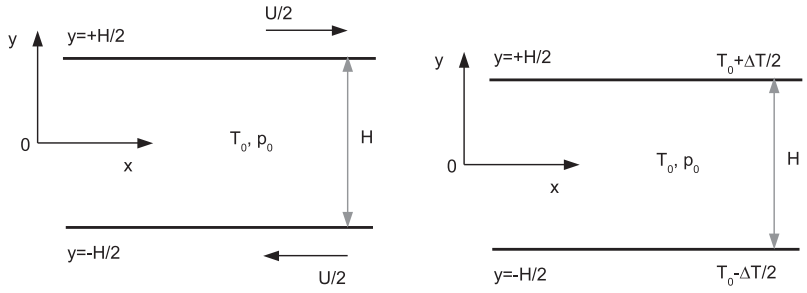

(a) Couette flow (b) Fourier flow

Fig. 1. Schematic of the Couette and Fourier flows between two parallel plates.

where c_α is the molecular velocity and $p_{0\alpha} = n_{0\alpha}kT_0$ is the partial pressure of species α.

When the perturbation functions h_α are known, the velocity and shear stress in Couette flow are $u_{\alpha x} = \sqrt{m/m_\alpha}\int h_\alpha c_{\alpha x} f_\alpha^0 dc_\alpha$ and $P_{\alpha xy} = \int h_\alpha c_{\alpha x} c_{\alpha y} f_\alpha^0 dc_\alpha$, respectively, while the deviated density, deviated temperature, and the heat flux in Fourier flow are $n_\alpha = \int h_\alpha f_\alpha^0 dc_\alpha, T_\alpha = \int h_\alpha(\frac{2}{3}c_\alpha^2 - 1) f_\alpha^0 dc_\alpha$, and $q_{\alpha i} = \sqrt{m/m_\alpha}\int h_\alpha c_{\alpha i}(c_\alpha^2 - \frac{5}{2}) f_\alpha^0 dc_\alpha$, respectively, where $f_\alpha^0 = \pi^{-3/2}\exp(-c_\alpha^2)$. The dimensionless macroscopic quantities of the binary gaseous mixture in Couette flow are defined as follows:

$$\begin{aligned} u_x(y) &= \frac{m_1 n_{01} u'_{1x} + m_2 n_{02} u'_{2x}}{n_0 m U} = \frac{C_0 m_1 u_{1x}(y) + (1-C_0) m_2 u_{2x}(y)}{m}, \\ P_{xy}(y) &= \frac{P'_{1xy} + P'_{2xy}}{2p_0\xi} = C_0 P_{1xy}(y) + (1-C_0) P_{2xy}(y), \end{aligned} \tag{9}$$

while those in Fourier flow are defined as follows:

$$\begin{aligned} n(y) &= \frac{n'_1 + n'_2}{n_0\xi} = C_0 n_1(y) + (1-C_0) n_2(y), \\ C(y) &= \frac{C' - C_0}{C_0\xi} = (1-C_0)[n_1(y) - n_2(y)], \\ T(y) &= \frac{n_{01} T'_1 + n_{02} T'_2}{n_0\xi} = C_0 T_1(y) + (1-C_0) T_2(y), \\ q_y(y) &= \frac{q'_{1y} + q'_{2y}}{p_0 v_0 \xi} = C_0 q_{1y}(y) + (1-C_0) q_{2y}(y). \end{aligned} \tag{10}$$

where $p_0 = n_0 kT_0$ is the equilibrium pressure of the mixture. Expressions for the macroscopic quantities of the binary gaseous mixture in the LBE can be given similarly.

3.3. Boundary conditions

The Maxwell diffuse-specular boundary condition is adopted to describe the gas-wall interaction. When molecules hit the plate, an a_α portion of them ($0 < a_\alpha \le 1$) are diffusely reflected, while the rest are specularly reflected. There is complete accommodation when the accommodation coefficient a_α is unitary. In this paper, if not otherwise specified, complete accommodation is assumed.

In the linearized Couette flow the boundary condition for the LBE has the following form

$$f_\alpha^{d+}(y = \pm 1/2) = (1 - a_\alpha) f_\alpha^{d-}(y = \pm 1/2) \pm a_\alpha m_\alpha v_x f_\alpha^M, \tag{11}$$

while that for the McCormack model is [4]

$$h_\alpha^+(y = \pm 1/2) = (1 - a_\alpha) h_\alpha^-(y = \pm 1/2) \pm a_\alpha \sqrt{\frac{m_\alpha}{m}} c_{\alpha x}, \tag{12}$$

where the superscripts + and − of the perturbation functions in Eqs. (11) and (12) refer to the outgoing and incoming molecules with respect to the plates' surfaces, respectively.

In the linearized Fourier flow the boundary condition for the LBE reads

$$\begin{aligned} f_\alpha^{d+}(y = \pm 1/2) &= (1 - a_\alpha) f_\alpha^{d-}(y = \pm 1/2) + a_\alpha [n_\alpha(y = \pm 1/2) \pm (m_\alpha v^2/2 - 1)] f_\alpha^M, \\ n_\alpha(y = \pm 1/2) &= \pm \tfrac{2\sqrt{m_\alpha \pi}}{n_{0\alpha}} \int\int f_\alpha^{d-}(y = \pm 1/2) v_y dv, \end{aligned} \tag{13}$$

while that for the McCormack model is [12]

$$\begin{aligned} h_\alpha^+(y = \pm 1/2) &= (1 - a_\alpha) h_\alpha^-(y = \pm 1/2) + a_\alpha \left[n_\alpha(y = \pm 1/2) \pm (c_\alpha^2/2 - 1) \right], \\ n_\alpha(y = \pm 1/2) &= \pm \tfrac{2}{\pi} \int h_\alpha^-(y = \pm 1/2) \exp(-c_\alpha^2) c_{\alpha y} dc_\alpha. \end{aligned} \tag{14}$$

3.4. Numerical techniques

The Boltzmann collision operators in the BE (3) and LBE (7) are solved by the fast spectral method (FSM) [14]. The main idea of the FSM is to expand the distribution function and collision operator into Fourier series, and handle the binary collision in a corresponding frequency space. The method can deal with highly rarefied gas flows, where the distribution function has large discontinuities. The number of discretized velocities can be large to capture the discontinuities, but the number of frequency components is relatively small, resulting in high computational accuracy and efficiency [15]. We discretize the three-dimensional molecular velocity space by $32 \times 64 \times 32$ points (the points are uniformly distributed in the v_x and v_z directions, while the discretization in the v_y direction is non-uniform, with most of them concentrating on $v_y \sim 0$ to capture the discontinuities in the molecular distribution function), while the corresponding frequency space is uniformly discretized by $32 \times 32 \times 32$ points.

When the Boltzmann collision operator is obtained, the LBE (7) is solved by an iterative scheme [14], where the spatial derivative is approximated by a second-order upwind finite-difference. The physical half-space $-1/2 \leqslant y \le 0$ is discretized by 50 points non-uniformly, with most points located near the plate to capture the velocity slip and temperature jump. The iterations terminate when the maximum relative difference (excluding the point $y = 0$) in macroscopic quantities (such as the velocity and shear stress in Couette flow, and the density, temperature, and heat flux in Fourier flow) between two consecutive steps is less than 10^{-5}.

The discrete velocity method [4] is used to solve the McCormack kinetic Eq. (8). To reduce computational effort, the $c_{\alpha z}$ variable is eliminated by introducing the reduced functions of h_α [16]: $\Phi_\alpha = \frac{1}{\sqrt{\pi}}\sqrt{\frac{m}{m_\alpha}}\int h_\alpha \exp(-c_{\alpha z}^2) dc_{\alpha z}$ and $\Psi_\alpha = \frac{1}{\sqrt{\pi}}\sqrt{\frac{m}{m_\alpha}}\int h_\alpha c_{\alpha z}^2 \exp(-c_{\alpha z}^2) dc_{\alpha z}$. The entire physical space is uniformly discretized into 400 points, and a first-order finite-difference is used to approximate the spatial derivative. The two-dimensional reduced molecular velocity space is discretized by 50×50 points according to Gaussian–Hermit quadrature. Grid-independence is checked with

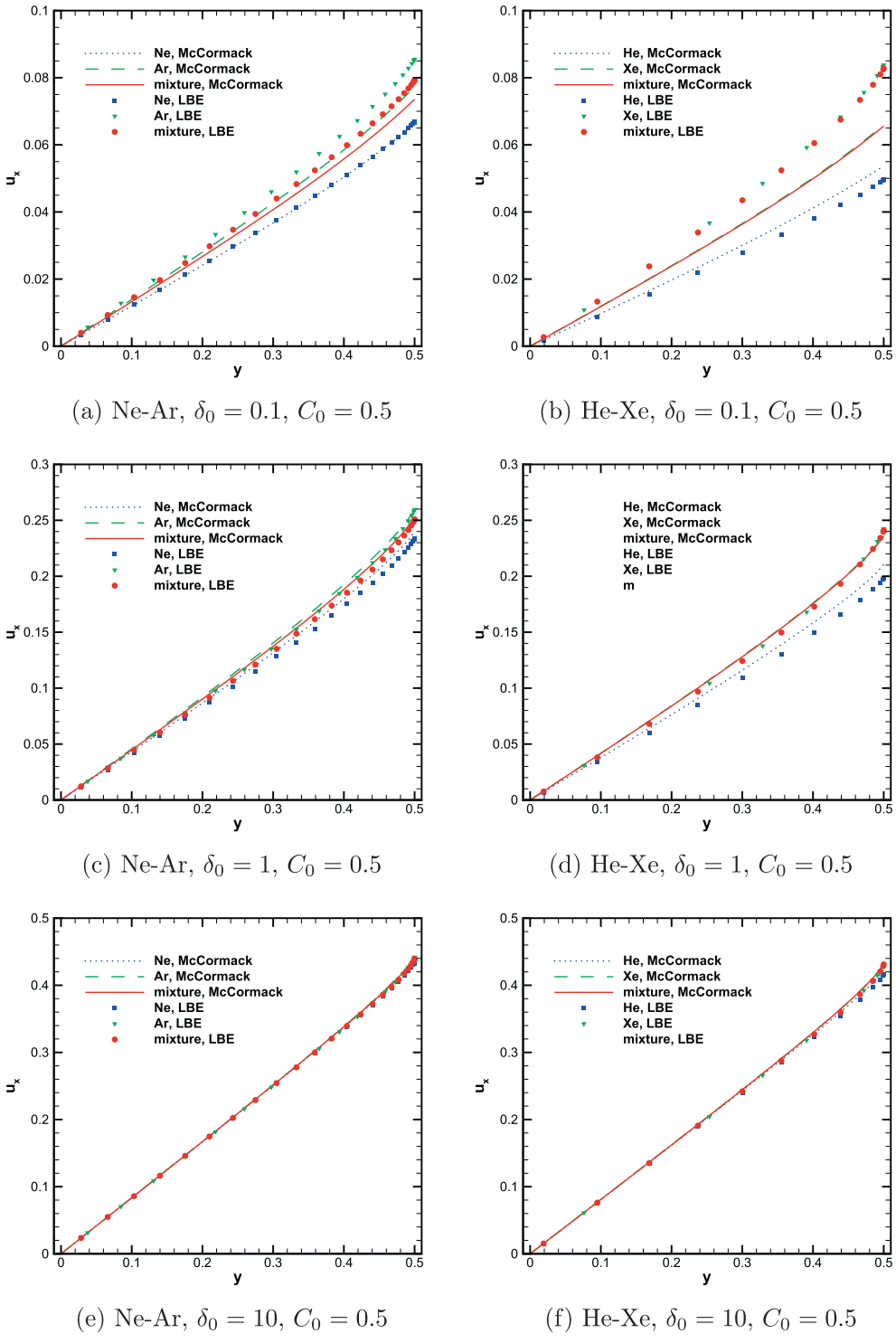

(a) Ne-Ar, $\delta_0 = 0.1$, $C_0 = 0.5$ (b) He-Xe, $\delta_0 = 0.1$, $C_0 = 0.5$

(c) Ne-Ar, $\delta_0 = 1$, $C_0 = 0.5$ (d) He-Xe, $\delta_0 = 1$, $C_0 = 0.5$

(e) Ne-Ar, $\delta_0 = 10$, $C_0 = 0.5$ (f) He-Xe, $\delta_0 = 10$, $C_0 = 0.5$

Fig. 2. Velocity profiles in the Couette flow of Ne–Ar and He–Xe gas mixtures with $C_0 = 0.5$.

a coarser grid of molecular velocity space 32×32 points for He–Xe mixture of $C_0 = 0.5$ and $\delta_0 = 0.1$ showing less than 1% difference in the macroscopic profiles. As we seek the steady-state solution the time-independent Eq. (8) is solved by the fixed point method. The convergence criterion $\int_{-1/2}^{1/2} |A^{l+1}/A^l - 1| < 10^{-10}$ is employed, where l is the iteration step, and $A = P_{xy}$ in the Couette flow and $A = q_y$ in the Fourier flow.

4. Numerical results

The binary gaseous mixtures Ne–Ar and He–Xe are chosen in this comparative study in order to investigate the influence of the molecular mass ratio. Three values of the molar concentration $C_0 = 0.1, 0.5$, and 0.9 are considered at three values of the rarefaction parameter $\delta_0 = 0.1, 1$, and 10. For Ne–Ar and He–Xe mixtures

Table 1
Velocities at $y = 0.5$ in the linearized Couette flow of a Ne–Ar mixture.

δ_0	u_{Ne}		u_{Ar}		u	
	McCormack	LBE	McCormack	LBE	McCormack	LBE
$C_0 = 0.1$						
0.1	0.0633	0.0621	0.0736	0.0785	0.0730	0.0776
1	0.2341	0.2257	0.2536	0.2509	0.2525	0.2496
10	0.4361	0.4320	0.4420	0.4397	0.4417	0.4393
$C_0 = 0.5$						
0.1	0.0663	0.0669	0.0773	0.0855	0.0736	0.0793
1	0.2399	0.2336	0.2598	0.2596	0.2531	0.2509
10	0.4377	0.4343	0.4435	0.4419	0.4416	0.4393
$C_0 = 0.9$						
0.1	0.0712	0.0745	0.0833	0.0960	0.0734	0.0784
1	0.2492	0.2453	0.2695	0.2720	0.2529	0.2501
10	0.4407	0.4380	0.4463	0.4454	0.4417	0.4393

Table 2
The mixture shear stress P_{xy} in the linearized Couette flow of a Ne–Ar mixture.

δ_0	$C_0 = 0.1$		0.5		0.9	
	McCormack	LBE	McCormack	LBE	McCormack	LBE
0.1	0.2601	0.2598	0.2576	0.2570	0.2594	0.2590
1	0.1689	0.1707	0.1675	0.1692	0.1685	0.1703
10	0.0415	0.0423	0.0414	0.0422	0.0415	0.0423

at an equilibrium temperature $T_0 = 300K$, the molecular diameter ratios are $d_2/d_1 = 1.406$ and 2.226, respectively, while the corresponding molecular mass ratios m_2/m_1 are 1.979 and 32.8. Both Couette and Fourier flows are characterized by the following rarefaction parameter [17]:

$$\delta_0 = \frac{Hp_0}{\mu v_0}, \tag{15}$$

where $\mu = \mu_1 + \mu_2$ is the viscosity of the mixture, see Appendix A.

4.1. Couette flow

The velocity in the Ne–Ar mixture with molar concentration $C_0 = 0.5$ at $\delta_0 = 0.1, 1$, and 10 is shown in the left column of Fig. 2. When $\delta_0 = 0.1$, the Ar gas velocity is different by 9% between the McCormack model and the LBE, while the difference in Ne is less than 1%. When $\delta = 1$, the difference in the Ar velocity quickly decreases, while that in the Ne velocity slightly increases. By $\delta = 10$, there are practically no differences in all the respective velocities. The influence of the molecular mass ratio on the velocity profile is observed by comparing the left (Ne–Ar) and right (He–Xe) columns in Fig. 2. It is clear that the larger the mass ratio, the greater the difference between the McCormack model and the LBE. For example, at $\delta_0 = 0.1$, the McCormack model underpredicts the velocity of Xe at the plate by about 24%.

The influence of the molar concentration C_0 on the gas velocity at the plate is summarized in Table 1. As C_0 varies from 0.1 to 0.9, the difference in Ar velocity between the McCormack model and the LBE increases from 6% to 13% when $\delta_0 = 0.1$. For $\delta_0 = 10$, this difference is less than 1% for all considered values of C_0. On the other hand, the relative difference in the Ne velocity between the two kinetic equations is less than 4% for all values of C_0 and δ_0: the maximum 4% is when $C_0 = 0.9$ and $\delta_0 = 0.1$.

The shear stresses P_{xy} in the Ne–Ar mixture are listed in Table 2 for different values of the molar concentration and the rarefaction parameter. Theoretically, the mixture shear stress has to be constant, but numerical results vary slightly across the channel. Therefore, the average shear stress $P_{xy}^{av} = \int_{-1/2}^{1/2} P_{xy} dy$ is presented. The maximum variation in the shear stress across the channel, $\max_i |(P_{xy}(i) - P_{xy}^{av})/P_{xy}^{av}|$, is less than 0.4%, which indicates the good numerical accuracy of both the FSM and the discrete velocity method. Good agreement between the McCormack model and the LBE is observed: the relative difference increases from 0.1% when $\delta_0 = 0.1$ up to 2% when $\delta_0 = 10$, for all molar concentrations. We have also calculated the shear stress of the He–Xe mixture with $C_0 = 0.5$. They are, respectively, 0.2163, 0.1482, and 0.0400 when $\delta_0 = 0.1, 1$, and 10 from the McCormack model, and 0.2150, 0.1491, and 0.0411 from the LBE. The relative difference in the shear stress in the He–Xe mixture between the two kinetic equations is slightly higher than that in the Ne–Ar mixture.

4.2. Fourier flow

The number density in the Ne–Ar mixture with $C_0 = 0.5$ when $\delta_0 = 0.1, 1$, and 10 is shown in the left column of Fig. 3. The difference in the Ne number density predicted by the McCormack model and the LBE reaches 31% when $\delta_0 = 0.1$. This difference decreases as the rarefaction parameter increases, with only 5% difference by $\delta_0 = 10$. Fig. 3 also shows that for mixtures with disparate molecular masses (i.e. He–Xe) the disagreement in the number density between the McCormack model and the LBE is larger than for the Ne–Ar mixture, especially at small values of the rarefaction parameter. The influence of the molar concentration on the number density is shown in Table 3. Large differences, i.e. 38% and 24%, are found in Ne and Ar, respectively, when $\delta_0 = 0.1$ and $C_0 = 0.1$. This difference is reduced when the molar concentration of Ne is increased: at $C_0 = 0.9$, the maximum differences in Ne and Ar are 22% and 3%, respectively.

The molar concentration C in the Ne–Ar and He–Xe mixtures, which is defined as the deviation of the concentration of the lighter species from its initial equilibrium state, is shown in Fig. 4. Positive values of C mean that the concentration of the lighter species increases near the hotter plate due to thermodiffusion. Although the McCormack model, in contrast to several other kinetic models such as the Hamel model [6], can describe the thermodiffusion phenomenon in gaseous mixtures, comparisons in Fig. 4 show that the McCormack model underestimates the thermodiffusion significantly when compared to the LBE. For instance, when $\delta_0 = 0.1$, the McCormack model underpredicts the molar concentration at the hotter plate by 40% and 67% for Ne–Ar and He–Xe mixtures, respectively. Even when $\delta_0 = 10$, the relative differences between the McCormack and LBE results are as high as 14% and 20% for Ne–Ar and He–Xe mixtures, respectively.

The temperature variation in the Ne–Ar mixture with $C_0 = 0.5$ when $\delta_0 = 0.1, 1$, and 10 is shown in the left column of Fig. 5. Good agreement between the McCormack model and the LBE is found when $\delta_0 = 10$. However, when $\delta_0 = 0.1$, the difference in the temperature results for Ne reaches 13%, while the difference for Ar is negligible. The influence of the molecular mass ratio on the temperature is seen by comparing the left and right columns of Fig. 5. As in Couette flow, the difference between the McCormack model and the LBE increases with the molecular mass ratio.

The influence of the molar concentration on the gas temperature at the hotter plate is shown in Table 4. When $\delta_0 = 0.1$, the maximum difference between results from the two kinetic equations. (18%) is found for Ne when $C_0 = 0.1$, and this reduces to 7% when $C_0 = 0.9$. So the difference between the two kinetic equations decreases as C_0 increases.

The heat flux in the Ne–Ar mixture is given in Table 5. As with the shear stress in Couette flow, here the average heat flux across the channel is reported. From Table 5 we see that the heat flux has its maximum value for the molar concentration $C_0 = 0.5$ for all rarefactions. The maximum difference between the McCormack model and the LBE results is about 2%. We have also calculated the heat flux in the

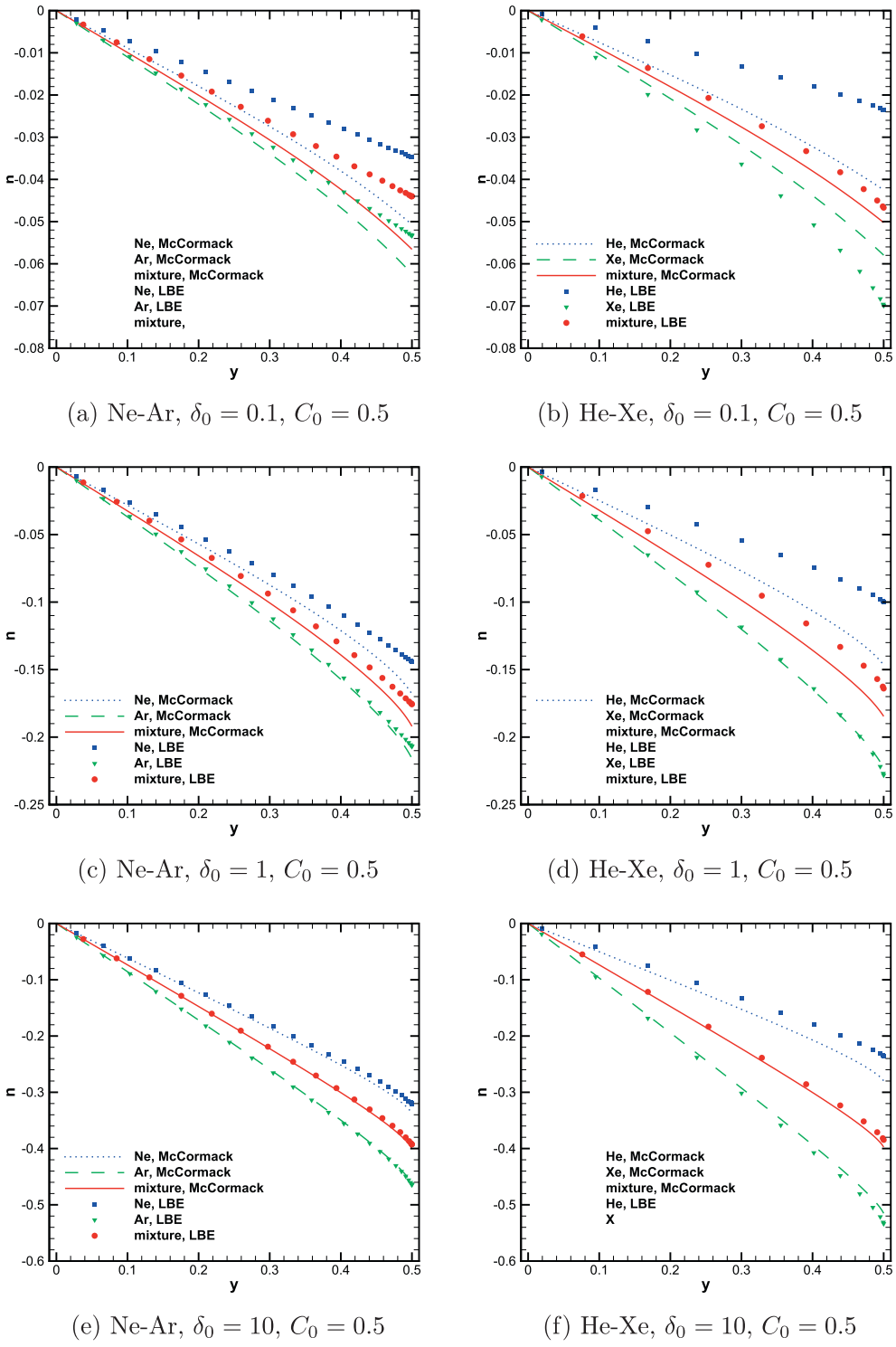

(a) Ne-Ar, $\delta_0 = 0.1$, $C_0 = 0.5$ (b) He-Xe, $\delta_0 = 0.1$, $C_0 = 0.5$

(c) Ne-Ar, $\delta_0 = 1$, $C_0 = 0.5$ (d) He-Xe, $\delta_0 = 1$, $C_0 = 0.5$

(e) Ne-Ar, $\delta_0 = 10$, $C_0 = 0.5$ (f) He-Xe, $\delta_0 = 10$, $C_0 = 0.5$

Fig. 3. The number density in the linearized Fourier flow of Ne–Ar and He–Xe gas mixtures.

He–Xe mixture with $C_0 = 0.5$. At $\delta = 0.1$, 1, and 10, heat fluxes from the McCormack model are 1.3012, 0.9839, and 0.3304, respectively, while the corresponding data from the LBE are 1.3121, 1.0314, and 0.3622. This means that the relative difference in the He–Xe mixture between the two models is greater than in the Ne–Ar mixture.

4.3. Effect of the incomplete accommodation

We studied the influence of the gas-wall interaction by simulating the incomplete accommodation. In the following, simulations of a Ne–Ar mixture with $C_0 = 0.5$ are carried out for both Couette and Fourier flows, where the accommodation coefficients for Ne and Ar are $a_{Ne} = 0.6$ and $a_{Ar} = 0.8$, respectively.

4.3.1. Couette flow with incomplete accommodation

The influence of the incomplete accommodation on the velocity can be seen by comparing data in Table 6 with those in Table 1. Clearly, the species velocities decrease with a decrease in the accommodation coefficient. Profiles of the shear stress are shown in Fig. 6. We find the shear stress of each species is quite different,

Table 3
The number density at $y = 0.5$ in the linearized Fourier flow of a Ne–Ar mixture.

δ_0	$-n_{Ne}$		$-n_{Ar}$		$-n$	
	McCormack	LBE	McCormack	LBE	McCormack	LBE
C_0 = 0.1						
0.1	0.0481	0.0296	0.0576	0.0434	0.0566	0.0420
1	0.1577	0.1296	0.1947	0.1796	0.1910	0.1746
10	0.3093	0.2877	0.4094	0.4038	0.3994	0.3922
C_0 = 0.5						
0.1	0.0507	0.0347	0.0624	0.0533	0.0566	0.0440
1	0.1680	0.1443	0.2159	0.2069	0.1920	0.1756
10	0.3375	0.3209	0.4631	0.4643	0.4003	0.3926
C_0 = 0.9						
0.1	0.0551	0.0428	0.0705	0.0684	0.0566	0.0454
1	0.1847	0.1667	0.2496	0.2476	0.1912	0.1748
10	0.3826	0.3731	0.5508	0.5612	0.3994	0.3919

and they are nearly constant when $\delta_0 = 0.1$, but vary significantly across the channel when $\delta_0 = 10$. The smaller the accommodation coefficient, the larger the variation of the shear stress of each species.

Shear stresses from McCormack simulations of the equal-mole Ne–Ar mixture with incomplete accommodation are 0.1503, 0.1119, and 0.0366 when $\delta_0 = 0.1$, 1, and 10, respectively, while the corresponding values from the LBE are 0.1500, 0.1125, and 0.0373. Compared to the data in Table 2, it is clear that the shear stress decreases with the accommodation coefficient. The relative difference (about 2%) between the results from the two kinetic equations remains the same as in the complete accommodation case.

4.3.2. Fourier flow with incomplete accommodation

The number density and temperature of each species and the mixture at the hot plate are presented in Table 6. The influence of incomplete accommodation can be seen by comparing the corresponding data in Tables 3 and 4. We find that the agreement between the McCormack model and the LBE is essentially improved when there is incomplete accommodation. For instance, with incomplete accommodation, the differences in the density of Ne and Ar when $\delta_0 = 0.1$ are reduced from 31% to 21%, and from 14% to 5%, respectively. For the temperature, the difference in Ne when $\delta_0 = 0.1$ is reduced from 13% to 7%, but that in Ar increases from 2% to 7%.

The influence of incomplete accommodation on the concentration is shown in Fig. 7. The absolute value of the concentration increases when the accommodation coefficient decreases, especially in the near free-molecular regime ($\delta_0 = 0.1$), and the agreement between the McCormack model and the LBE becomes better for incomplete accommodation.

The absolute value of the heat flux is shown in Fig. 8. As with the shear stress in Couette flow, the heat flux of each species is not constant in the slip-flow regime ($\delta_0 = 10$). When $\delta_0 = 0.1$, 1, and 10, heat fluxes from the McCormack model with incomplete accommodation are 0.3009, 0.2491, and 0.1126, respectively, while

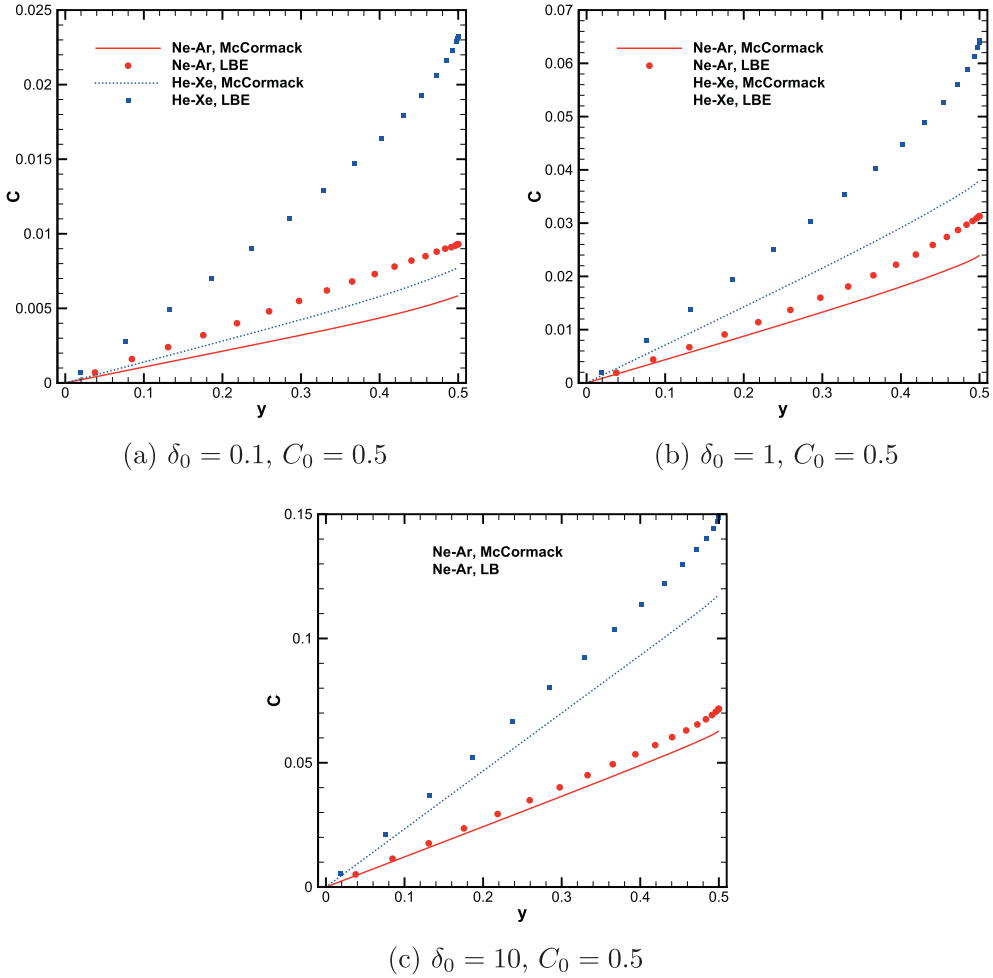

(a) $\delta_0 = 0.1$, $C_0 = 0.5$ (b) $\delta_0 = 1$, $C_0 = 0.5$

(c) $\delta_0 = 10$, $C_0 = 0.5$

Fig. 4. Concentration of the lighter species in the linearized Fourier flow of Ne–Ar and He–Xe gas mixtures.

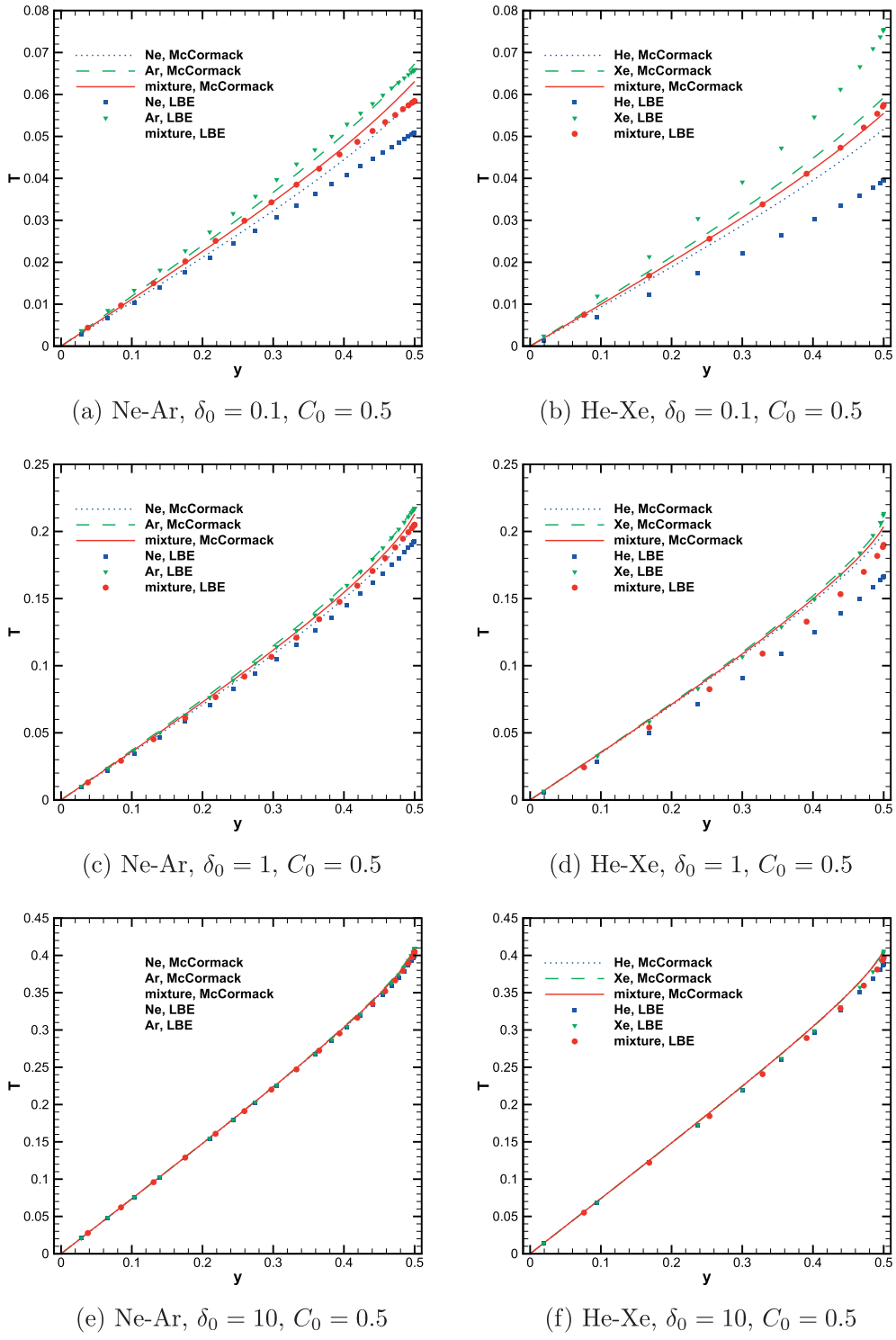

(a) Ne-Ar, $\delta_0 = 0.1$, $C_0 = 0.5$ (b) He-Xe, $\delta_0 = 0.1$, $C_0 = 0.5$

(c) Ne-Ar, $\delta_0 = 1$, $C_0 = 0.5$ (d) He-Xe, $\delta_0 = 1$, $C_0 = 0.5$

(e) Ne-Ar, $\delta_0 = 10$, $C_0 = 0.5$ (f) He-Xe, $\delta_0 = 10$, $C_0 = 0.5$

Fig. 5. Temperature profiles in the linearized Fourier flow of Ne–Ar and He–Xe gas mixtures with $C_0 = 0.5$.

those from the LBE are 0.3013, 0.2522, and 0.1154. Compared to the data in Table 5 when $C_0 = 0.5$ and there is complete accommodation, the heat flux decreases with a decrease in the accommodation coefficient, but the difference between the McCormack model and the LBE results remains unchanged.

4.4. The limit of the linearized approach

In the above sections, numerical results obtained from the McCormack model are compared with results from the LBE because the McCormack model requires the deviations of the gas parameters from their equilibrium values to be small. Therefore, it is useful to determine the applicability limit of this linearized approach, especially for the case of the heat flux through a gaseous mixture with large wall-temperature ratios. We carried out simulations on the heat transfer between two parallel plates with the temperature differences $\Delta T/T_0 = 0.6$ and 1, which leads to the large temperature ratios $T_H/T_C = 1.8$ and 3, respectively. Under these conditions, the assumption of a small deviation of the plate's temperature from its equilibrium value (i.e. $\Delta T \ll T_0$) is not fulfilled.

Table 4
Temperature at $y = 0.5$ in the linearized Fourier flow of a Ne–Ar gas mixture.

δ_0	T_{Ne}		T_{Ar}		T	
	McCormack	LBE	McCormack	LBE	McCormack	LBE
C_0 = 0.1						
0.1	0.0569	0.0466	0.0640	0.0579	0.0633	0.0568
1	0.2020	0.1863	0.2136	0.2065	0.2124	0.2045
10	0.4045	0.3974	0.4093	0.4052	0.4088	0.4044
C_0 = 0.5						
0.1	0.0589	0.0509	0.0673	0.0659	0.0631	0.0584
1	0.2056	0.1928	0.2205	0.2171	0.2131	0.2050
10	0.4065	0.4003	0.4127	0.4093	0.4096	0.4048
C_0 = 0.9						
0.1	0.0622	0.0577	0.0727	0.0779	0.0632	0.0597
1	0.2106	0.2018	0.2296	0.2303	0.2125	0.2047
10	0.4081	0.4033	0.4154	0.4132	0.4088	0.4043

Table 5
Total heat flux q_y in the linearized Fourier flow of a Ne–Ar gas mixture.

δ_0	$C_0 = 0.1$		$C_0 = 0.5$		$C_0 = 0.9$	
	McCormack	LBE	McCormack	LBE	McCormack	LBE
0.1	0.5430	0.5450	0.5589	0.5607	0.5446	0.5462
1	0.4058	0.4128	0.4172	0.4252	0.4069	0.4146
10	0.1364	0.1381	0.1397	0.1424	0.1368	0.1397

Table 6
Velocity u_x in Couette flow, and number density n with temperature T in Fourier flow, at $y = 0.5$ in the Ne–Ar gas mixture with $C_0 = 0.5$. The accommodation coefficients are $a_{Ne} = 0.6$ and $a_{Ar} = 0.8$.

δ_0	McCormack	LBE	McCormack	LBE	McCormack	LBE
	u_{Ne}		u_{Ar}		u	
0.1	0.0328	0.0337	0.0571	0.0641	0.0489	0.0539
1	0.1492	0.1448	0.2098	0.2106	0.1894	0.1885
10	0.3851	0.3799	0.4100	0.4077	0.4017	0.3984
	$-n_{Ne}$		$-n_{Ar}$		$-n$	
0.1	0.0255	0.0201	0.0463	0.0450	0.0359	0.0325
1	0.0992	0.0833	0.1688	0.1604	0.1340	0.1219
10	0.2740	0.2582	0.4035	0.3967	0.3387	0.3274
	T_{Ne}		T_{Ar}		T	
0.1	0.0292	0.0277	0.0506	0.0546	0.0399	0.0411
1	0.1211	0.1130	0.1781	0.1767	0.1496	0.1449
10	0.3311	0.3220	0.3661	0.3608	0.3486	0.3414

In this case the full BE is solved by the FSM [14] for the equal-mole Ne–Ar gas mixture with complete accommodation at three values of the rarefaction parameter. Good agreement in the number density is observed in Fig. 9 when $\delta_0 = 0.1$ and 10, except in a small region in the vicinity of the wall (especially in the slip-flow regime and near the colder plate).

For the comparison of temperature profiles between the McCormack model and the BE, we note that near the free-molecular regime the gas temperature tends to a constant value $T_{FM} = \sqrt{T_C T_H}$. However, in the linearized approach we calculate the temperature deviation from its reference value $T_0 = (T_C + T_H)/2$. Therefore, to compare the temperature obtained from the McCormack model with the results from the BE when $\delta_0 = 0.1$, we take T_{FM} as the reference temperature. From Fig. 10b it is clear that the use of T_{FM} as the reference temperature makes the comparison meaningful, and the temperature profiles from the McCormack model display good agreement with these from the BE. This is not the case when the mean temperature T_0 is chosen as the reference value, and large shifts between the two kinetic model results are observed, see Fig. 10a. In the slip-flow regime ($\delta_0 = 10$), however, choosing the mean temperature T_0 as the reference value (Fig. 10c), instead of the free-molecular value T_{FM} (Fig. 10d) enables a meaningful comparison, and perfect agreement between the two kinetic equations is found.

The dimensionless heat fluxes obtained from the McCormack model, the LBE, and the BE are compared in Table 7. Good agreement of the McCormack results with the solution of the BE, of the order of 4%, is found at $\Delta T/T_0 = 0.6$. However, for the temperature difference, $\Delta T/T_0 = 1$, the deviation between the McCormack model and the BE increases, to 9%.

5. Conclusion

Plane Couette and Fourier flows of binary gaseous mixture have been simulated using the McCormack kinetic model and the linearized Boltzmann equation, over a wide range of the molar concentration and rarefaction parameter. Two gaseous mixtures, one with similar molecular masses (Ne–Ar) and the other with disparate molecular masses (He–Xe), have been considered. Our numerical results showed that when only the shear stress in Couette flow and the heat flux in Fourier flow are required, the McCormack model can be used, as the differences in the results from the two kinetic models are within 2%. However, difference in other

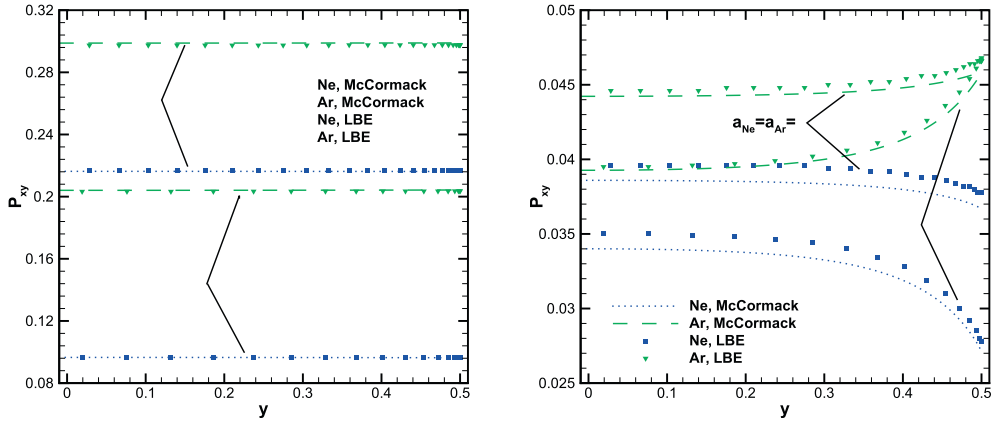

(a) $\delta_0 = 0.1$ (b) $\delta_0 = 10$

Fig. 6. The shear stress in the linearized Couette flow of an equal-mole Ne–Ar gas mixture with complete ($a_{Ne} = a_{Ar} = 1.0$) and incomplete ($a_{Ne} = 0.6, a_{Ar} = 0.8$) accommodation.

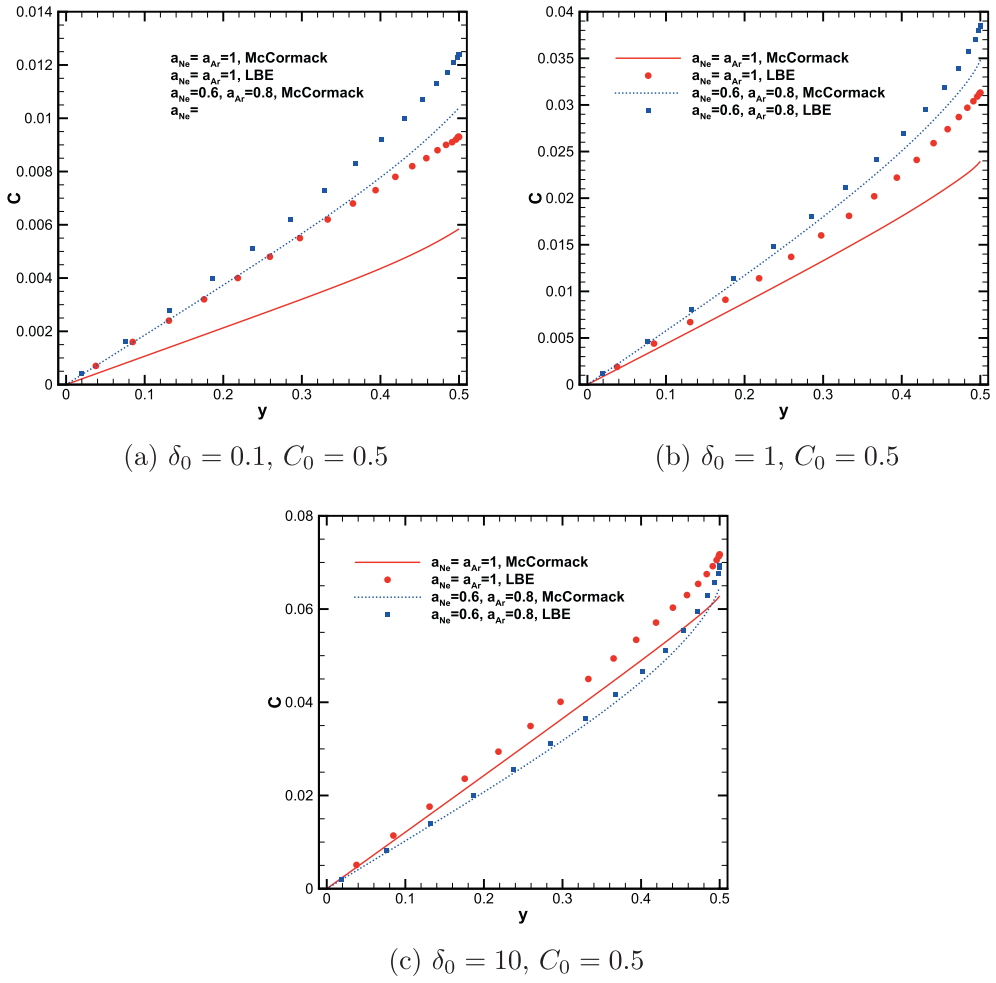

(a) $\delta_0 = 0.1$, $C_0 = 0.5$ (b) $\delta_0 = 1$, $C_0 = 0.5$

(c) $\delta_0 = 10$, $C_0 = 0.5$

Fig. 7. Concentration of the lighter species in the linearized Fourier flow of Ne–Ar gas mixture: influence of the accommodation coefficient.

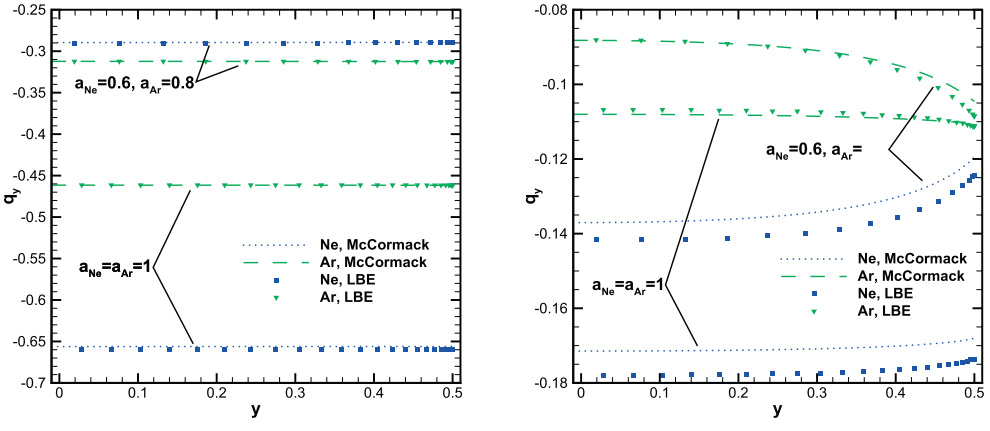

(a) $\delta_0 = 0.1$ (b) $\delta_0 = 10$.

Fig. 8. The heat flux in the Fourier flow of an equal-mole Ne–Ar gas mixture with complete ($a_{\mathrm{Ne}} = a_{\mathrm{Ar}} = 1.0$) and incomplete ($a_{\mathrm{Ne}} = 0.6, a_{\mathrm{Ar}} = 0.8$) accommodation coefficients.

macroscopic quantities, such as the deviated density, velocity, deviated temperature can be large, especially in transitional and free-molecular flows. For example, the McCormack model could underestimate the deviated concentration (due to thermodiffusion of the lighter species) by 67% in Fourier flow of He–Xe when $\delta_0 = 0.1$. Our numerical results also showed that the differences in macroscopic quantities from the McCormack model and the linearized Boltzmann equation increase with the molecular mass ratio (for fixed rarefaction parameter and molar concentration). On the other hand, if the molecular mass ratio and the rarefaction parameter are fixed, the difference increases with an increase in the molar concentration of the heavier species. The fact that the

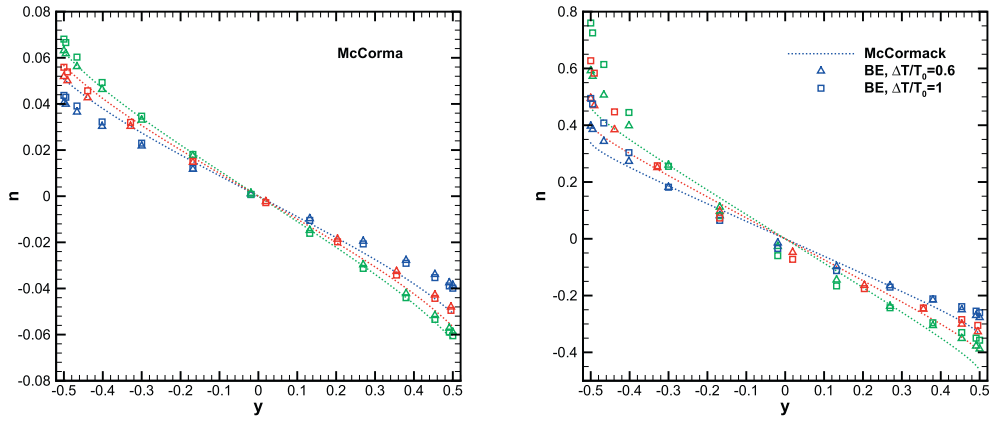

(a) Density n, $\delta_0 = 0.1$ (b) Density n, $\delta_0 = 10$.

Fig. 9. The number density variation in the Fourier flow of a Ne–Ar gas mixture with $C_0 = 0.5$. Ne: in blue, Ar: in green, mixture: in red. (For interpretation of the references to colour in this figure legend, the reader is referred to the web version of this article.)

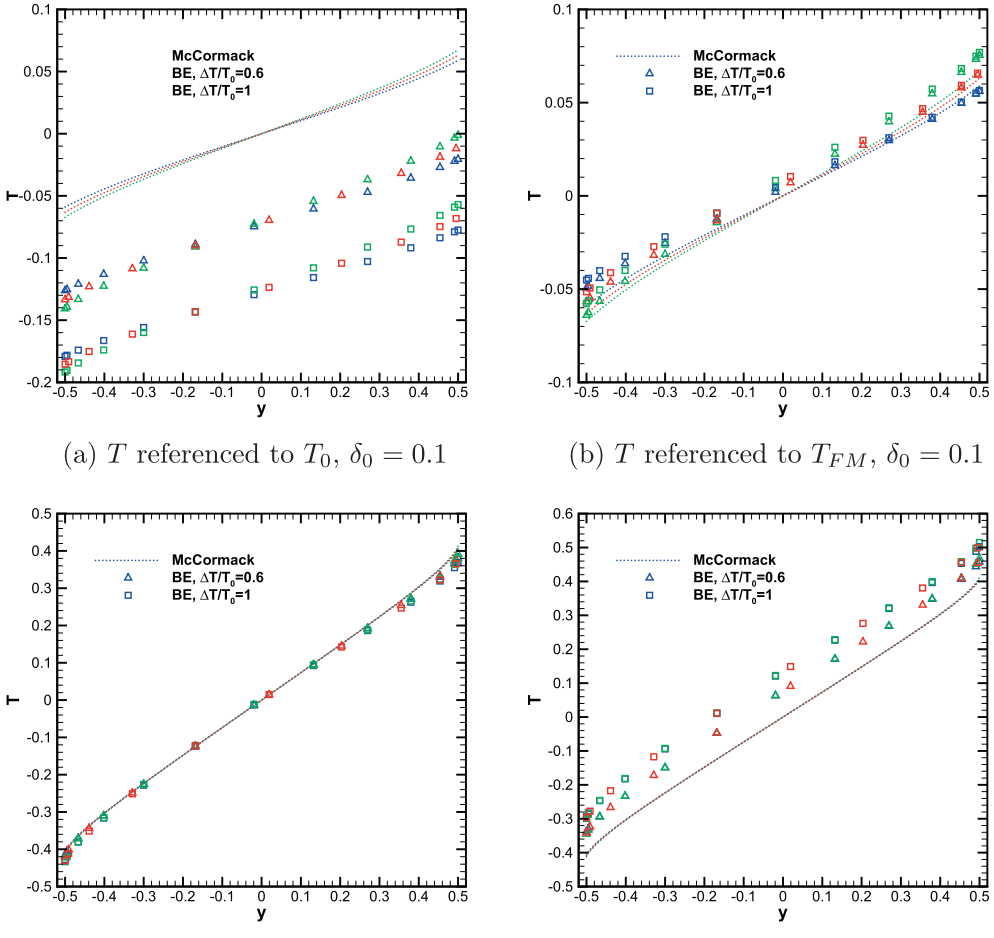

(a) T referenced to T_0, $\delta_0 = 0.1$ (b) T referenced to T_{FM}, $\delta_0 = 0.1$

(c) T referenced to T_0, $\delta_0 = 10$. (d) T referenced to T_{FM}, $\delta_0 = 10$.

Fig. 10. The temperature variation in the Fourier flow of a Ne–Ar gas mixture with $C_0 = 0.5$. Ne: in blue, Ar: in green, mixture: in red. (For interpretation of the references to colour in this figure legend, the reader is referred to the web version of this article.)

McCormack model is not accurate for highly rarefied gas is because the collision term of McCormack model only recovers the relaxation rate of low order momentum (such as pressure tensor, heat flux), while at small value of δ_0 the relaxation of higher order moments is important.

Finally, we investigated the applicability of the McCormack model in nonlinear Fourier flow. We found that the McCormack model can provide temperature profiles in relatively good agreement with those from the Boltzmann equation, even for large differences in the plates' temperatures. However, the reference

Table 7
The heat flux q_y in a Ne–Ar gas mixture with $C_0 = 0.5$ for different wall-temperature ratios.

δ_0	$\Delta T/T_0 \ll 1$		$\Delta T/T_0 = 0.6$	$\Delta T/T_0 = 1$
	McCormack	LBE	BE	BE
0.1	0.5589	0.5607	0.5423	0.5059
1	0.4172	0.4252	0.4168	0.3927
10	0.1397	0.1424	0.1454	0.1425

temperature has to be adapted to the rarefaction parameter: in the slip-flow and hydrodynamic regimes the arithmetic mean of the two plates' temperatures should be chosen as the reference value, while near the free-molecular regime the geometric average (complete accommodation) should be chosen. In the intermediate region, either the arithmetic or geometric temperature can be used. As far as the heat flux is concerned, the use of the McCormack model is acceptable, with a maximum error of about 9% even when the temperature ratio of the two plates is 3.

Acknowledgement

M.T. Ho and I. Graur thank the Labex MEC project (ANR-10-LABX-0092) and the A*MIDEX project (ANR-11-IDEX-0001-02), funded by the "Investissements d'Avenir" French Government program managed by the French National Research Agency (ANR), for their support. This work is also financially supported by the UK's Engineering and Physical Sciences Research Council (EPSRC) under Grants EP/I036117/1, EP/I011927/1, and EP/K038621/1.

Appendix A. The McCormack collision term

The collision term of the McCormack model [7] has the following form:

$$\begin{aligned} L_{\alpha\beta}h = & -\gamma_{\alpha\beta}h_\alpha + \gamma_{\alpha\beta}n_\alpha \\ & + 2\sqrt{\tfrac{m_\alpha}{m}}\left[\gamma_{\alpha\beta}u_{\alpha i} - \upsilon^{(1)}_{\alpha\beta}(u_{\alpha i}-u_{\beta i}) - \tfrac{\upsilon^{(2)}_{\alpha\beta}}{2}\left(q_{\alpha i} - \tfrac{m_\alpha}{m_\beta}q_{\beta i}\right)\right]c_{\alpha i} \\ & + \left[\gamma_{\alpha\beta}T_\alpha - 2\tfrac{m_{\alpha\beta}}{m_\beta}(T_\alpha - T_\beta)\upsilon^{(1)}_{\alpha\beta}\right](c_\alpha^2 - \tfrac{3}{2}) \\ & + 4\left[\left(\gamma_{\alpha\beta} - \upsilon^{(3)}_{\alpha\beta}\right)P_{\alpha xy} + \upsilon^{(4)}_{\alpha\beta}P_{\beta xy}\right]c_{\alpha x}c_{\alpha y} \\ & + 2\left[\left(\gamma_{\alpha\beta} - \upsilon^{(3)}_{\alpha\beta}\right)P_{\alpha yy} + \upsilon^{(4)}_{\alpha\beta}P_{\beta yy}\right]\left(c_{\alpha y}^2 - \tfrac{1}{2}c_{\alpha x}^2 - \tfrac{1}{2}c_{\alpha z}^2\right) \\ & + \tfrac{4}{5}\sqrt{\tfrac{m_\alpha}{m}}\left[\left(\gamma_{\alpha\beta} - \upsilon^{(5)}_{\alpha\beta}\right)q_{\alpha i} + \upsilon^{(6)}_{\alpha\beta}\sqrt{\tfrac{m_\beta}{m_\alpha}}q_{\beta i} - \tfrac{5}{4}\upsilon^{(2)}_{\alpha\beta}(u_{\alpha i} - u_{\beta i})\right]c_{\alpha i}(c_\alpha^2 - \tfrac{5}{2}), \end{aligned} \tag{A.1}$$

where $\alpha, \beta = 1, 2, i = x, y$ for Couette and Fourier flows, respectively, and $\upsilon^{(i)}_{\alpha\beta}$ are defined as following

$$\begin{aligned} \upsilon^{(1)}_{\alpha\beta} &= \tfrac{16}{3}\tfrac{m_{\alpha\beta}}{m_\alpha}n_\beta\Omega^{11}_{\alpha\beta}, \\ \upsilon^{(2)}_{\alpha\beta} &= \tfrac{64}{15}\left(\tfrac{m_{\alpha\beta}}{m_\alpha}\right)^2 n_\beta\left[\Omega^{12}_{\alpha\beta} - \tfrac{5}{2}\Omega^{22}_{\alpha\beta}\right], \\ \upsilon^{(3)}_{\alpha\beta} &= \tfrac{16}{5}\tfrac{m^2_{\alpha\beta}}{m_\alpha m_\beta}n_\beta\left[\tfrac{10}{3}\Omega^{11}_{\alpha\beta} + \tfrac{m_\beta}{m_\alpha}\Omega^{22}_{\alpha\beta}\right], \\ \upsilon^{(4)}_{\alpha\beta} &= \tfrac{16}{5}\tfrac{m^2_{\alpha\beta}}{m_\alpha m_\beta}n_\beta\left[\tfrac{10}{3}\Omega^{11}_{\alpha\beta} - \Omega^{22}_{\alpha\beta}\right], \\ \upsilon^{(5)}_{\alpha\beta} &= \tfrac{64}{15}\left(\tfrac{m_{\alpha\beta}}{m_\alpha}\right)^3\tfrac{m_\alpha}{m_\beta}n_\beta\left[\Omega^{22}_{\alpha\beta} + \left(\tfrac{15}{4}\tfrac{m_\alpha}{m_\beta} + \tfrac{25}{8}\tfrac{m_\beta}{m_\alpha}\right)\Omega^{11}_{\alpha\beta} - \tfrac{1}{2}\tfrac{m_\beta}{m_\alpha}\left(5\Omega^{12}_{\alpha\beta} - \Omega^{13}_{\alpha\beta}\right)\right], \\ \upsilon^{(6)}_{\alpha\beta} &= \tfrac{64}{15}\left(\tfrac{m_{\alpha\beta}}{m_\alpha}\right)^3\left(\tfrac{m_\alpha}{m_\beta}\right)^{3/2}n_\beta\left[-\Omega^{22}_{\alpha\beta} + \tfrac{55}{8}\Omega^{11}_{\alpha\beta} - \tfrac{5}{2}\Omega^{12}_{\alpha\beta} + \tfrac{1}{2}\Omega^{13}_{\alpha\beta}\right], \end{aligned} \tag{A.2}$$

where

$$m_{\alpha\beta} = \frac{m_\alpha m_\beta}{m_\alpha + m_\beta} \tag{A.3}$$

is the reduced mass of the binary mixture. Note that $\Omega^{(i,j)}_{\alpha\beta}$ in Eq. (A.2) represents the omega integral [18], which for the case of the HS model is defined as [18]

$$\Omega^{(i,j)}_{\alpha\beta} = \frac{(j+1)!}{8}\left[1 - \frac{1+(-1)^i}{2(i+1)}\right]\left(\frac{\pi kT}{2m_{\alpha\beta}}\right)^{1/2}(d_\alpha + d_\beta)^2. \tag{A.4}$$

Finally, the parameters $\gamma_{\alpha\beta}$ are proportional to the collision frequency between species α and β and appear in the collision term (A.1) only in the combinations $\gamma_1 = \gamma_{11} + \gamma_{12}$ and $\gamma_2 = \gamma_{21} + \gamma_{22}$, so one has only to define γ_1 and γ_2. The collision frequencies and the viscosity can be related in the same manner as in the Shakhov kinetic equation [19,20,4]:

$$\gamma_\alpha = \frac{p_{0_\alpha}}{\mu_\alpha}, \tag{A.5}$$

where $p_{0_\alpha} = n_{0_\alpha}kT_0$ is the equilibrium partial pressure and μ_α is the partial viscosity given as

$$\mu_\alpha = p_{0_\alpha}\frac{S_\beta + \upsilon^{(4)}_{\alpha\beta}}{S_\alpha S_\beta - \upsilon^{(4)}_{\alpha\beta}\upsilon^{(4)}_{\beta\alpha}}, \quad S_\alpha = \upsilon^{(3)}_{\alpha\alpha} - \upsilon^{(4)}_{\alpha\alpha} + \upsilon^{(3)}_{\alpha\beta}, \quad \text{and} \quad \beta \neq \alpha. \tag{A.6}$$

Our numerical simulations are carried out using dimensionless quantities. The dimensionless omega integrals are defined as follows

$$\Omega^{*(i,j)}_{\alpha\beta} = \Omega^{(i,j)}_{\alpha\beta}\left[\frac{1}{4}\sqrt{\frac{\pi kT}{2m_{12}}}d_1^2\right]^{-1}. \tag{A.7}$$

As examples, the dimensional and dimensionless form of $\Omega^{(1,1)}_{\alpha\beta}$ are

$$\begin{aligned} \Omega^{(1,1)}_{\alpha\beta} &= \tfrac{1}{4}\sqrt{\tfrac{\pi kT}{2m_{\alpha\beta}}}(d_\alpha + d_\beta)^2, \\ \Omega^{*(1,1)}_{\alpha\beta} &= \sqrt{\tfrac{m_{12}}{m_{\alpha\beta}}}\left(\tfrac{d_\alpha + d_\beta}{d_1}\right)^2. \end{aligned} \tag{A.8}$$

The dimensionless $\upsilon^{(n)}_{\alpha\beta}$ functions (A.2) are defined as follows:

$$\upsilon^{*(i)}_{\alpha\beta} = \upsilon^{(i)}_{\alpha\beta}\left[\frac{1}{4}\sqrt{\frac{\pi kT}{2m_{12}}}d_1^2 n_1\right]^{-1}. \tag{A.9}$$

As examples, the dimensional and dimensionless form of $\upsilon^{(1)}_{\alpha\beta}$ are

$$\begin{aligned} \upsilon^{(1)}_{\alpha\beta} &= \tfrac{16}{3}\tfrac{m_{\alpha\beta}}{m_\alpha}n_\beta\Omega^{(1,1)}_{\alpha\beta}, \\ \upsilon^{*(1)}_{\alpha\beta} &= \tfrac{16}{3}\tfrac{m_{\alpha\beta}}{m_\alpha}\tfrac{n_\beta}{n_1}\Omega^{*(1,1)}_{\alpha\beta}. \end{aligned} \tag{A.10}$$

We note that γ_α, S_α have the same dimension as $\upsilon^{(i)}_{\alpha\beta}$, so we use the same reference quantity to obtain the dimensionless expressions for these functions.

References

[1] Y. Onishi, On the behavior of a slightly rarefied gas mixture over plane boundaries, Z. Angew. Math. Phys. (ZAMP) 37 (1986) 573–596.
[2] D. Valougeorgis, Couette flow of a binary gas mixture, Phys. Fluids 31 (3) (1988) 521–524.
[3] C.E. Siewert, Couette flow for a binary gas mixture, J. Quant. Spectr. Rad. Tran. 70 (2001) 321–332.
[4] F. Sharipov, L.M.G. Cumin, D. Kalempa, Plane Couette flow of binary gaseous mixture in the whole range of the Knudsen number, Eur. J. Mech. B/Fluids 23 (2004) 899–906.
[5] R.D.M. Garcia, C.E. Siewert, The McCormack model for gas mixtures: plane Couette flow, Phys. Fluids 17 (3) (2005) 037102.1–037102.6.
[6] B.B. Hamel, Kinetic model for binary gas mixture, Phys. Fluids 8 (3) (1965) 418–425.
[7] F.J. McCormack, Construction of linearized kinetic models for gaseous mixture and molecular gases, Phys. Fluids 16 (1973) 2095–2105.

[8] R.D.M. Garcia, C.E. Siewert, Couette flow of a binary mixture of rigid-sphere gases described by the linearized Boltzmann equation, Eur. J. Mech. B/Fluids 27 (2008) 823–836.
[9] S. Kosuge, K. Aoki, S. Takata, Heat transfer in a gas mixture between two parallel plates: finite-difference analysis of the Boltzmann equation, in: T.J. Bartel, M.A. Gallis, (Eds.), Rarefied Gas Dynamics, vol. 585, 22nd Int. Symp., AIP Conference Proc., Melvile, 2001, pp. 289–296.
[10] R.D.M. Garcia, C.E. Siewert, The McCormack model for gas mixtures: heat transfer in a plane channel, Phys. Fluids 16 (9) (2004) 3393–3402.
[11] R.D.M. Garcia, C.E. Siewert, Heat transfer between parallel plates: an approach based on the linearized Boltzmann equation for a binary mixture of rigid-sphere gases, Phys. Fluids 19 (2) (2007) 027102.1–027102.7.
[12] F. Sharipov, L.M.G. Cumin, D. Kalempa, Heat flux through a binary gaseous mixture over the whole range of the Knudsen number, Phys. A 378 (2007) 183–193.
[13] J. Kestin, K. Knierim, E.A. Mason, B. Najafi, S.T. Ro, M. Waldman, Equilibrium and transport properties of the noble gases and their mixture at low densities, J. Phys. Chem. Ref. Data 13 (1) (1984) 229–303.
[14] L. Wu, J. Zhang, J.M. Reese, Y. Zhang, A fast spectral method for the boltzmann equation for monoatomic gas mixture, J. Comput. Phys. 298 (2015) 602–621.
[15] L. Wu, J.M. Reese, Y.H. Zhang, Solving the Boltzmann equation by the fast spectral method: application to microflows, J. Fluid Mech. 746 (2014) 53–84.
[16] S. Naris, D. Valougeorgis, F. Sharipov, D. Kalempa, Discrete velocity modelling of gaseous mixture flows in mems, Superlattices Microst. 35 (3–6) (2004) 629–643.
[17] F. Sharipov, V. Seleznev, Data on internal rarefied gas flows, J. Phys. Chem. Ref. Data 27 (3) (1998) 657–706.
[18] J.H. Ferziger, H.G. Kaper, Mathematical Theory of Transport Processes in Gases, North-Holland Publishing Company, Amsterdam, 1972.
[19] E.M. Shakhov, Generalization of the Krook kinetic relaxation equation, Fluid Dyn. 3 (5) (1968) 95–96.
[20] F. Sharipov, D. Kalempa, Gaseous mixture flow through a long tube at arbitrary Knudsen number, J. Vac. Sci. Technol. A 20 (3) (2002) 814–822.